Behavior of piled raft during 2D trap door tunnel excavation

Nagoya Institute of Technology, Researcher Member ○H. M. Shahin
Nagoya Institute of Technology, Professor Member Teruo Nakai, Feng Zhang
Nagoya Institute of Technology, Graduate Students Student Member Yusuke Tabata, Eriko Nakahara

ABSTRACT

Two-dimensional model tests have been performed to investigate tunneling induced piled raft behaviors using trap door apparatus. The corresponding finite element simulations are also carried out using the elastoplastic subloading t_{ij} model. In this research, the effect of tunnel excavation on the piled raft is investigated varying the pile length for the same soil cover. It is revealed that the distance between the pile tip and the tunnel crown changes the patterns of both axial force and bending moment of the piles. The numerical simulation with the constitutive model shows very good agreement with the results of the model tests.

1. LAYOUT OF MODEL TESTS AND ANALYSES

Fig.1 represents the 2D trap door apparatuses for piled raft used in the model tests. The reference [2] described the details of the apparatus. The model ground consists of the mass of aluminum rods, having diameters of 1.6mm and 3.0mm mixed in a ratio of 3:2 in weight. The unit weight of the aluminum rod mass is 20.4kN/m^3, and the length is 50mm. After the installation of the pile in the ground, tunnel excavation is performed descending block F until 4mm. Strain gauges are placed externally on both sides of the piles to measure axial force and bending moments of the piles during tunnel excavation. The size and stiffness of the piled raft are obtained from the real field condition considering the similarity ratio of 1:100. The Young's modulus of the pile is E=1.063×10^5 kPa/cm. The applied dead load is equivalent to the load of a twenty-stories building (stress of 392kPa at base level) assuming a similarity ratio of 1:100. The tests are conducted for 32cm soil cover (D/B=3.0), and D_p/B equals 2.0 and 1.0. Here, D is the soil cover, B (=8cm) is the width of trap door and D_p is the vertical distance between the pile tip and the tunnel block. Fig. 2 shows the mesh used in the finite element analyses. The finite element anlyses using FEMtij-2D and elasto-plastic subloading t_{ij} model [1] have been carried out with the same scale of the model tests considering plane strain drained conditions. Isoparametric 4-noded elements are used in the mesh. Both vertical sides of the mesh are free in the vertical direction, and the bottom face is fixed. The pile is modeled as elastic element in the analyses. Elastoplastic joint element is used as an interface element between the ground and the foundations taking the friction angle δ=18°. To simulate the tunnel excavation, vertical displacement is applied up to 4mm to the nodes that correspond to the tunnel block. Model parameters for the aluminum rod mass are shown in Table 1, and with these parameters stress strain relations under constant minor principal stress are shown in Fig. 3.

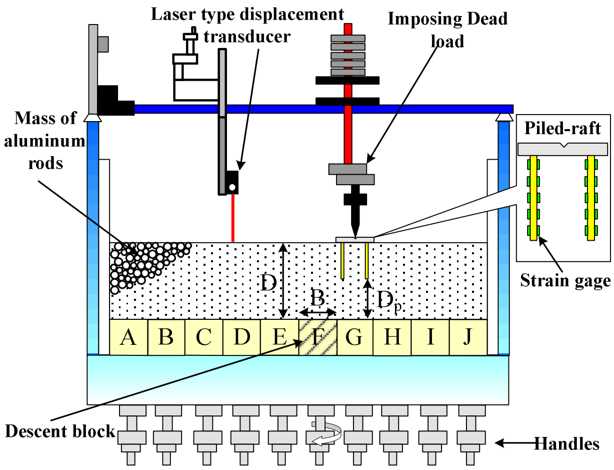

Fig.1. Trap door apparatus

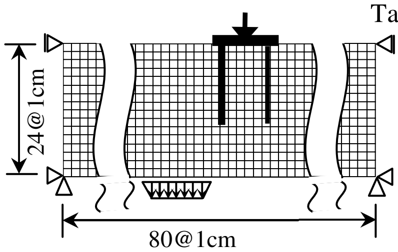

Fig.2. Finite element mesh

Table 1. Parameter of aluminum rod

λ	0.008
κ	0.004
N (e_{NC} at p=98kPa & q=0kPa)	0.30
$R_{CS}=(\sigma_1/\sigma_3)_{CS(comp.)}$	1.80
β	1.20
ν_e	0.20
a	1300

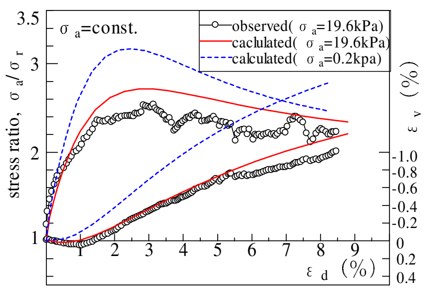

Fig.3 Stress-strain curves for the mass of aluminum rods

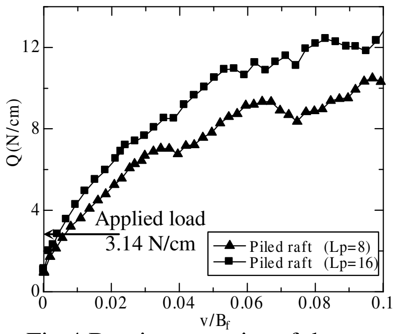

Fig.4 Bearing capacity of the piled raft in the model ground

2. RESULTS AND DISCUSSIONS

Fig.5 shows the induced axial force due to tunnel excavation in the front pile (pile nearer the tunnel block). Fig.6 indicates the same in the rear pile (pile located further from the tunnel block). Figs.5(a) and 6(a) represent the results of the model tests, and Figs.5(b) and 6(b) illustrate the computed results obtained from finite element analyses. The vertical axis represents the length of the pile. The legend represents the amount of applied displacements (amount of descendent of the tunnel block). It is seen in these figures that the axial force in the front pile slightly increases for D_p/B=2.0. It implies that the settlement of the front pile is slightly larger than that of the surrounding ground, which develops a little negative shaft friction. On the other hand, the axial force significantly decreases in the front pile for D_p/B=1.0. As the ground settlement is larger than the pile settlement in the region of the upper part of the front pile, positive shaft friction develops around at that region of the pile that causes the reduction of axial force by stress relaxation due to tunneling. It is also noticed that the reduction of the axial force near the pile tip is smaller than that of the upper part. The reason for this formation is – as the pile tip is somewhat closer to the tunnel

Key words: Tunnel excavation, Piled raft, Axial force, Bending moment, Finite element analyses
Contact address: Nagoya Institute of Technology, Gokiso-cho, Showa-ku, Nagoya 466, Japan, Phone &Fax-052-735-7157

crown the difference of the settlements between the ground and pile tip area is very small. The maximum reduction of the axial force in the front pile is about 8% of the ultimate bearing capacity of the pile (Fig.4). The results in Fig.6 (rear pile) are completely opposite of the results of the front pile due to the load transfer from the front pile and different shaft friction. In the rear pile for D_p/B=2.0 the axial force decrease, while it increase for D_p/B=1.0. It indicates that ground settlement is larger than that of the rear pile for D_p/B=2.0, and it is opposite in the case of D_p/B=1.0. The maximum increase of the axial force in the rear pile is about 4% of the ultimate bearing capacity. Therefore, it can be said that the distance between the pile tip and the tunnel crown is an important factor which controls the pattern of the axial force. The numerical simulation well captures the profiles of the tunneling induced axial force.

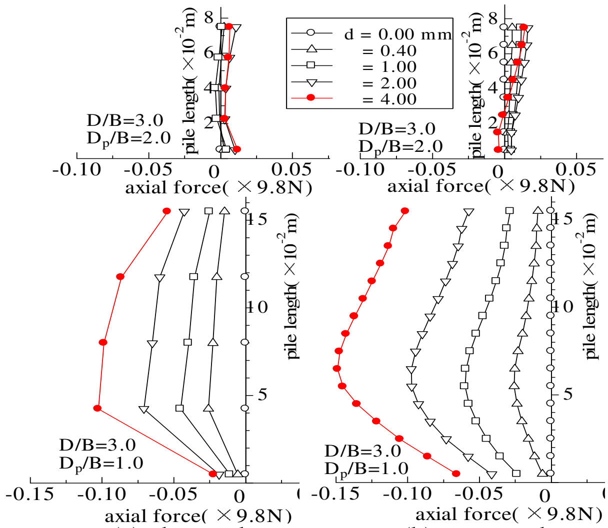

(a) observed (b) computed

Fig. 5 Tunneling induced axial force (front pile)

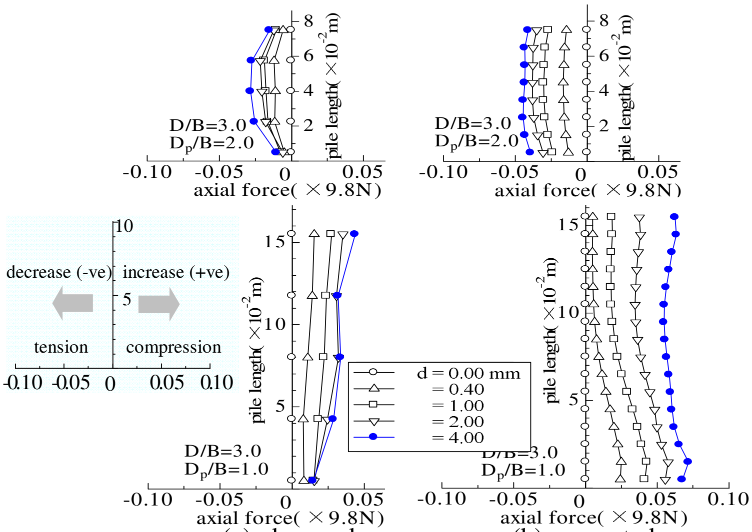

(a) observed (b) computed

Fig. 6 Tunneling induced axial force (rear pile)

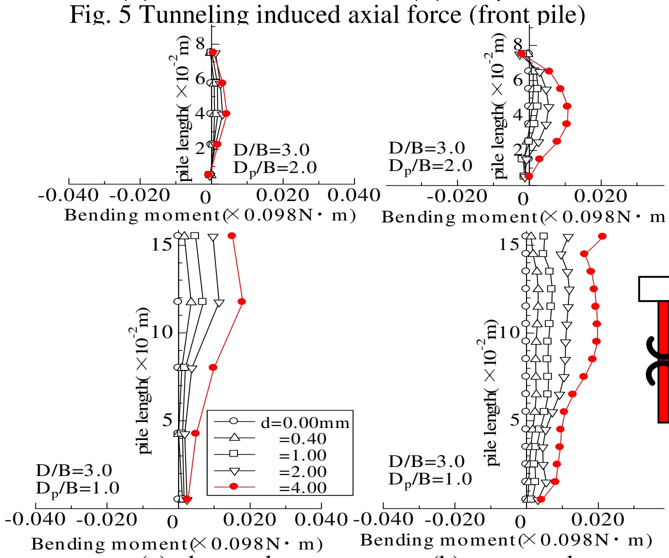

(a) observed (b) computed

Fig. 7 Tunneling induced bending moment (front pile)

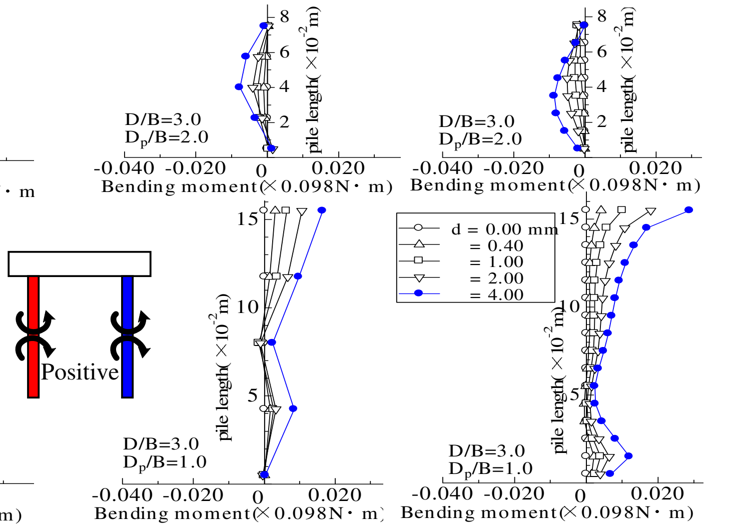

(a) observed (b) computed

Fig. 8 Tunneling induced bending moment (rear pile)

Figs. 7 and 8 show the induced bending moments on the front pile and rear pile due to tunnel excavation, respectively. Figs.7(a) and 8(a) represent the results of the model tests, and Figs. 7(b) and 8(b) illustrate the computed results. It is seen in the figures that bending moments develops due to the tunnel excavation, and its magnitude increases with the volume of excavation. The maximum bending moment occurs almost at the upper part of the front piles, while the rear pile experiences the maximum bending moment at the pile head. It is observed that the induced bending moments are larger for D_p/B=1.0 than that for D_p/B=2.0. It is also noticed that the pattern of the induced moment is different in the rear pile for D_p/B=2.0, which indicates the dependency of bending moment of the pile on the distance between the pile tip and the tunnel crown. The numerical analyses can perfectly capture the results of the model tests.

3 CONCLUSIONS

The distance between the pile tip and the crown of the tunnel plays an important role on the piled raft behavior. During tunnel excavation the axial force of the pile changes due to stress relaxation and change of shaft friction. The numerical analysis can well simulate the results of the model test for the tunneling induced piled raft behavior. Therefore, it can easily be said that the FEMtij-2D can be used to predict pile behavior in tunneling properly.

REFERENCES

1) Nakai, T., Hinokio, M. (2004): A simple elastoplastic model for normally and over consolidated soils with unified material parameters. *Soils and Foundations*, 44(2): 53-70. 2) Shahin, H. M., Nakai, T., Hinokio, M., Kurimoto, T., and Sada, T. (2004): Influence of surface loads and construction sequence on ground response due to tunneling, *Soils and Foundation*, 44(2), 71-84.